WATTMETERS

The wattmeter is an instrument which measures the average power P_0 entering a one-port. Under periodic conditions, P_0 is defined according to the following relationship:

$$P_0 = \frac{1}{T_1}\int_{t_A - T_1}^{t_A} v(t)i(t)dt \tag{1}$$

where $i(t)$ denotes the instantaneous current entering the port, $v(t)$ represents the instantaneous voltage across the port, and T_1 the period of the instantaneous power $p(t) = v(t)i(t)$. Under non-periodic conditions, Eq. (1) can be generalized by introducing the limit for T_1 tending to infinity. Equation (1) suggests a method for measuring the average power P_0 by applying the product of the input signals $v(t)$ and $i(t)$ to a linear time invariant (LTI) circuit whose impulse response $h(t)$ is shown in Fig. 1-a (1). Recalling the modulus of the Fourier transform $H(fT_1)$ of $h(t)$ (Fig. 1-b), when the condition $fT_1 = k$, with k integer, is satisfied, only the direct component P_0 of the instantaneous power is present at the output and it can be measured easily. In order to avoid this synchronisation requirement, a low pass filter (LPF) that properly attenuates all the alternate spectral components is normally used instead of the circuit with impulse response $h(t)$. The input conditioning circuits are necessary in order to convert the input signals both in type and amplitude so that they can be compatible with the multiplier to optimize the multiplier performance and to insulate the operator from the measurement section when needed. These circuits, together with the multiplier and the LPF, characterize the sensitivity, the bandwidth and the accuracy of the instrument; accuracy and sensitivity are also influenced by the instrument which measures P_0.

The electrodynamic wattmeter is an electromechanical implementation of the block diagram of Fig. 2. In fact, the instantaneous operating torque of the moving system is proportional to the product of the instantaneous currents in the fixed and moving coils. The effect of the couples

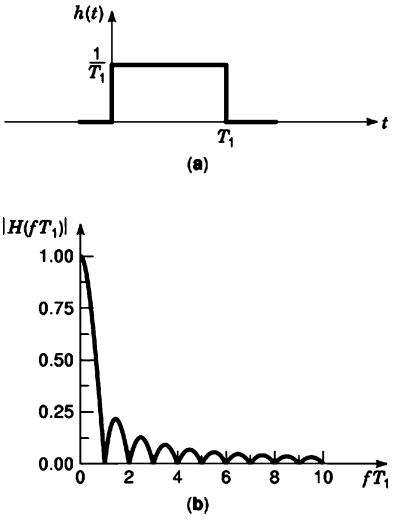

Figure 1. Impulse response (a) and its Fourier transform in modulus (b).

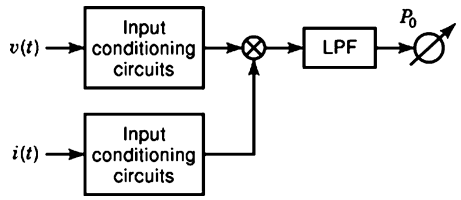

Figure 2. Block diagram of the wattmeter.

that oppose the motion (the restoring torque, the mechanical and electromagnetic damping torques, and the inertial torque of the moving system) is equivalent to a low-pass filter with a natural frequency on the order of 1 Hz. This instrument is particularly suitable for ac power measurements at line frequency and usually has an uncertainty of 0.5% at full scale. Precision electrodynamic wattmeters, having an uncertainty lower than 0.01% at line frequency, are also available, along with wideband wattmeters characterized by a frequency range up to a few kilohertz and uncertainty of 0.1%. Other techniques of multiplication were recently introduced (2) and some of them have been implemented in these instruments. One of them is the quarter-square technique. When both the quantities at the output of the conditioning circuits are currents, P_0 can be derived by measuring two root mean square (rms) values. In fact, by recalling the relationship:

$$i_1 i_2 = \frac{1}{4}[(i_1 + i_2)^2 - (i_1 - i_2)^2] \tag{2}$$

when the currents i_1 and i_2 to be multiplied are a function of the quantities that the instantaneous power depends on, the average power can be deduced from the difference of the rms values at the output of two thermal converters to which the quantities $(i_1 + i_2)$ and $(i_1 - i_2)$ are applied to (3–5). However, the most common multiplier technique used in average power measurement is time-division (6–10). Both accuracy and bandwidth featured by commercial instruments using this technique do not substantially differ from those of the best electrodynamic instruments; the dc output is normally applied to a digital voltmeter in order to obtain a digital output.

The integral in Eq. (1) can be approximated by a weighted sum of the product of successive N samples of $v(t)$ and $i(t)$:

$$\overset{a}{P}_k = \sum_{i=0}^{N-1} a_i v(t_{k-i})i(t_{k-i}) \tag{3}$$

where the integer k identifies a generic discrete output ${}^{a}P_k$, t_{k-i} is the ith sampling instant and a_i the value of the weighting function (11, 12). This equation leads to a power meter implemented according to the block diagram of Fig. 3: the outputs of the two input conditioning circuits are simultaneously sampled through a sampling time generator (STG), digitized and latched; the acquisition process is controlled by a digital signal processor (DSP). The two digital values are then acquired by the DSP to estimate the average power in real time. In a digital environment the multiplication does not present particular accuracy problems when a 32 bit floating-point DSP is used; therefore the measurement accuracy is influenced by both the adopted

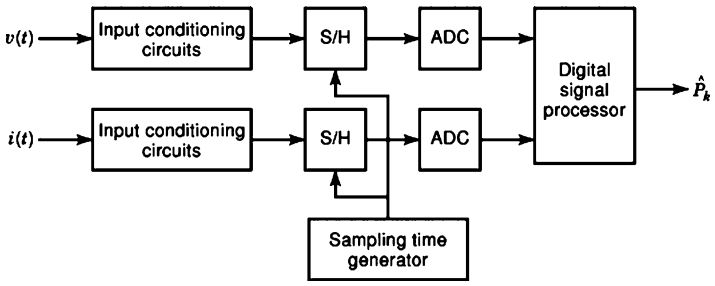

Figure 3. Block diagram of the sampling wattmeter.

sampling strategy and the filtering algorithms, along with the characteristics of the S/H-ADC (sample/hold, analog to digital converter) circuits, in particular by the frequency response of the S/Hs when they operate in the sample mode and by the resolution of the ADCs. The adopted sampling strategies are either of an equally spaced type (which can be divided into synchronous, quasi-synchronous and asynchronous) or a random asynchronous one. The latter represents a convenient solution when a large bandwidth and a high resolution are both required and relatively long measurement times are acceptable. The errors arising from the sampling strategy and the filtering procedures will be dealt with in the following sections separately from those associated with the input conditioning circuits.

Clearly, a power instrument based on Eq. (1) or (3) can also be used to implement the measurement of the rms value of each input signal.

The instruments described by the previous block diagrams can be also defined as transmission-type wattmeters since they are designed to be connected between a source and a load. Another type of wattmeter is the absorption type, which utilizes a power sensor to terminate the transmission line in a prefixed load (usually 50 Ω) and convert the dissipated power into a dc value which is then measured. Absorption-type wattmeters can be classified according to the type of power sensor (thermistor, thermocouple or diode) (13). These instruments can measure power values ranging from less than one nW up to some tens of W in the frequency range from dc up to some tens of GHz.

EQUALLY-SPACED SAMPLING WATTMETERS

If the N samples of Eq. (3) are taken at equally spaced instants T_s we can write:

$$t_{k-i} = \tau_0 + (k-i)T_s \tag{4}$$

where τ_0 is the shift between the initial sampling instant and the time origin of both $v(t)$ and $i(t)$. The minimum value of the time interval T_s depends on which is the greater between the acquisition time of the S/H-ADC devices and the processing time of the digital hardware. Since the uncertainty arising from digital multiplication can be neglected, Eq. (3) can be rewritten as follows:

$$^{a}P_k = \sum_{i=0}^{N-1} a_i\, p(t_{k-i}) \tag{5}$$

The periodic instantaneous power $p(t)$ can be represented by the Fourier series:

$$p(t) = \sum_{q=-\infty}^{+\infty} P_q e^{j2\pi q\, f_1 t} = P_0 + \sum_{\substack{q=-\infty \\ q\neq 0}}^{+\infty} P_q e^{j2\pi q\, f_1 t} \tag{6}$$

where $f_1 = 1/T_1$, $P_{-q} = P_q^*$ (P_q^* being the conjugate of P_q), and P_0 is the mean value of $p(t)$, i.e. the value of the measurand. By substituting Eqs. (6) and (4) into Eq. (5) we can write:

$$\begin{aligned} ^{a}P_k &= \sum_{q=-\infty}^{+\infty} P_q \sum_{i=0}^{N-1} a_i e^{j2\pi q\, f_1 t_{k-i}} \\ &= P_0 \sum_{i=0}^{N-1} a_i + \sum_{\substack{q=-\infty \\ q\neq 0}}^{+\infty} P_q e^{j2\pi q\, f_1(\tau_0 + kT_s)} H(q\, f_1 T_s) \end{aligned} \tag{7}$$

where:

$$H(fT_s) = \sum_{i=0}^{N-1} a_i e^{-j2\pi i\, fT_s} \tag{8}$$

is the frequency response of the finite impulse response (FIR) filter. The filter has a periodic response of period f_s; moreover, for $fT_s = u$, with u an integer, it results in $H(fT_s) = \sum_{i=0}^{N-1} a_i$. In order to obtain a unity scale factor in Eq. (7), the sum of the N coefficients a_i must be unity. Plainly, the coefficients a_i must be selected to obtain a frequency response which adequately attenuates the contribution to $^{a}P_k$ of each spectral component of $p(t)$. By assuming $a_i = 1/N$ (i.e. a rectangular window) we obtain the well-known Dirichlet-Kernel formula:

$$H(fT_s) = e^{-j\pi\, fT_s (N-1)} \frac{\mathrm{sinc}(N\, fT_s)}{\mathrm{sinc}(fT_s)}, \tag{9}$$

where the sinc function is defined as follows: $\mathrm{sinc}(x) = \sin(\pi x)/(\pi x)$. The frequency response of the FIR filter used is therefore a periodic function that assumes a unity value for fT_s integer and null values for $fT_s = r/N$, r being an integer which is not a multiple of N. Fig. 4 shows the shape of $|H(fT_s)|$ when $N = 10$ (this low value of N was chosen only for the sake of simplicity). Therefore, if a synchronous sampling strategy is used in which $f_1 T_s$ coincides with one of the zeroes of $H(fT_s)$, it follows that:

$$f_1 T_s = \frac{r}{N} \tag{10}$$

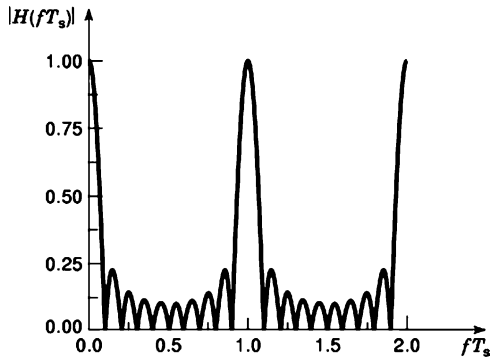

Figure 4. Frequency response in modulus of a rectangular window FIR filter with $N = 10$.

where r is a positive integer with no common submultiple with N, and only the spectral components of $p(t)$ whose harmonic order is an integer multiple of N contribute to the output (14–16). In fact, when $q = zN$ (z integer) in Eq. (7), we obtain:

$$\overset{a}{P}_0 = P_0 + \sum_{\substack{z=-\infty \\ z\neq 0}}^{+\infty} (-1)^{zr(N-1)} P_{zN} e^{j2\pi zN\, f_1 \tau_0}. \qquad (11)$$

The output ${}^aP_0$ is a constant and therefore becomes independent of k. The instrument bandwidth, referred to $p(t)$, becomes equal to $(N-1)\ f_1$; in fact, the first spectral component of $p(t)$ that gives a contribution to ${}^aP_0$ is the $N\ f_1$ one ($z = 1$). The quantities Ts and N in Eq. (10) can be independently selected provided that both signals are under steady-state conditions in the observation (or summation) interval NT_s. This interval, in which the N samples are taken, is also called the response time of the instrument. According to Eq. (10), this interval must be equal to an integer number of periods T_1 ($NT_s = rT_1$); therefore one of the input signals must drive the sampling time generator in order to synchronize the sampling time interval Ts with the period T_1. This is the most common solution adopted in commercial digital wattmeters. The frequency bandwidth (from dc to some hundreds of kHz) is obviously much greater than that of the traditional instruments based on the analog multiplication, and the accuracy is usually less than 0.1%.

If instead of the synchronization condition (Eq. 10) the following one is imposed:

$$|H(q\ f_1 T_s)| \leq \frac{1}{N} \qquad (12)$$

for any $q \neq zN$, the contribution to ${}^aP_k$ of the each corresponding spectral component qf_1 is not zero, as occurs in the synchronous sampling, but can be neglected if N is adequately high. Since Eq. (11) is still approximately valid, this sampling strategy is called quasi-synchronous (17). It can be shown (18) that, on the hypothesis of $f_1 T_s < 0.5$, Eq. (12) is verified when:

$$|NT_s - r_1 T_1| \leq T_s \quad for\ \ f_1 T_s < 0.5 \qquad (13)$$

where r_1 is the nearest integer to NT_s/T_1. In the quasi-synchronous case the value of N must therefore be adjusted so that the observation interval NT_s results close enough to an integer number of periods T_1 in order to satisfy Eq. (13). A prototype implementing this procedure featured an uncertainty of less than ±50 ppm in the frequency range 50 Hz to 1 kHz (19).

On the contrary, in the asynchronous case the product fT_s can assume any value; therefore the bandwidth is limited by the periodicity of the function $H(\ fT_s)$, i.e. fs, and the FIR filter must be selected in such a way to minimize $|H(\ fT_s)|$ within this interval (20).

RANDOM SAMPLING WATTMETERS

The need for synchronization to overcome the bandwidth limitations of the equally spaced sampling strategy may restrict the possible applications of the wattmeters. In fact, synchronisation can be conveniently used only when dealing with strictly periodic waveforms, while many applications of practical interest must dealt with almost periodic "multitone" signals, which are characterized by a discrete spectrum with nonharmonically related frequencies of the spectral components. Asynchronous sampling may also be more convenient in strictly periodic cases whenever synchronisation is a difficult task, either because the signals have a very broad spectrum or because the period is relatively long. The bandwidth of a wattmeter based on an asynchronous equally spaced sampling strategy is limited by the conversion time of the ADC; on the other hand, high resolution and short conversion time are two opposite requirements of an ADC. To build an asynchronous wattmeter whose bandwidth is not limited by the sampling frequency, two different random strategies (or more precisely pseudo-random since the mean sampling time is constant) have been proposed. The first one is defined by the expression (20):

$$t_{k-i} = \tau_0 + (k - i + X_{k-i})T_s \qquad (14)$$

where any sampling instant t_{k-i} is given by the sum of a periodic component $(k-i)T_s$ (k and i are integers) and a random one $X_{k-i}T_s$ (Fig. 5-a); the previously introduced quantity T_s (Eq. 4) is not correlated with any spectral component of the instantaneous power (i.e. this sampling strategy is of an asynchronous type), while $X_{k-i}$is the $(k-i)^{th}$ of a set of random independent variables having a continuous uniform distribution in the interval 0 to $\pm b$. It is noteworthy that Eq. (14) includes, as a special case, the equally spaced sampling strategy (Eq. 4). Under the assumption of $b = 0.5$, the successive sampling instants are distributed in consecutive non overlapping intervals equal to T_s. Since the distance between two consecutive sampling instants can be small without limitation, while the time interval between the first and the last of a consecutive triplet of samples can never be smaller than T_s, this strategy has the drawback of requiring a pair of S/H-ADC for each input channel.

In the other random strategy, called recursive random sampling strategy (21), every sampling instant t_{k-i} is obtained by adding to the preceding one t_{k-i-1} a predetermined constant lag T_s plus a random increment $X_{k-i}T_s$ (Fig. 5-b):

$$t_{k-i} = t_{k-i-1} + (1 + X_{k-i})T_s \qquad (15)$$

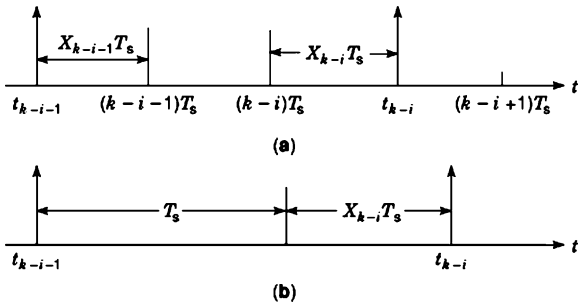

Figure 5. Sampling instants of a non-recursive (a) and a recursive (b) random sampling technique.

where $X_{k-i}$is the $(k-i)^{th}$ of a set of random independent variables having continuous uniform distribution in a prefixed interval 0 to b. The lag T_s has been devised so that the time interval between two successive samples is never smaller than T_s. Therefore, if its value is not less than the maximum data acquisition and processing time of the digital hardware used, a real time instrument can be realized by using only one S/H-ADC for each channel.

PERFORMANCE ANALYSIS OF THE SAMPLING WATTMETERS

By substituting Eqs. (14) or (15) and (6) into Eq. (5), we obtain the output quantity ${}^{a}P_k(\tau_0, \overline{X}_k)$, which is a function of the index k marking any output state of the instrument, of the shift τ_0 between the initial sampling instant and the time origin of $p(t)$, and of the vector of the successive N sampling random variables $\overline{X}_k = \{X_k, X_{k-1}, \ldots X_{k-N+1}\}$. The incidental quantities k and τ_0 occur as nuisance parameters because they locally condition the evaluation of ${}^{a}P_k(\tau_0, \overline{X}_k)$ by restricting it to the choice of a particular pair of values of k and τ_0. To eliminate the influence of these nuisance parameters, we can follow the Bayesian approach (22) by regarding any pair of possible values (k, τ_0) as a realization of a bivariate random variable (k, τ_0), with "a priori" probability distribution which must be selected by their intrinsic relationship to the prior information available. As far as k is concerned, it should be considered that every output state of the instrument has an equal chance of being selected; therefore, the enumerable sets of the labels, in general with $2h+1$ values, which mark the sequence of the output states of the instrument can be treated as a discrete random variable, uniformly distributed within the whole time interval in which these states are available. As far as τ_0 is concerned, we must distinguish between the synchronous sampling techniques and the asynchronous ones. In the asynchronous cases, the sampling time generator of Fig. 4 is not controlled by any input signal; therefore any realization of τ_0 is independent of the instantaneous power $p(t)$ and, since it is strictly related to the turn-on instant of the instrument, it belongs to a continuous set of possible equiprobable values distributed within any time interval. In the synchronous sampling technique, τ_0 depends on the synchronizing circuit that generates the sequence of the sampling instants as a function of one of the input signals; as a consequence, τ_0 is a function not only of the synchronizing circuit used but also of $p(t)$. If we want to take into account all possible states of τ_0, we should have to foresee all the possible synchronizing operations for the same unknown signal and establish the possible functional relations which connect τ_0 to the signal itself. Obviously, this is practically utopian and it is convenient to simulate an equivalent configuration in which τ_0 may be assumed as a realization of a continuous set of values distributed within some time interval T. To sum up, the "a priori" ignorance concerning the nature of the parameter τ_0 can be overcome in both techniques by postulating a uniform distribution in a generic time interval T (23, 24).

An appropriate characterization of the output uncertainty of the sampling wattmeters can be obtained by evaluating the statistical parameters of the output ${}^{a}P_k$, i.e. the mean value $\mathrm{E}\{{}^{a}P_k\}$ and the mean square error $\mathrm{E}\{({}^{a}P_k - P_0)^2\}$. To incorporate all the possible *a priori* chances and also to avoid the influence of the conventional time origin on the instrument performance, the number $2h+1$ of the output states, and the excursion T of the initial shift must be sufficiently large and theoretically must tend to infinite. Therefore we consider the asymptotic statistic parameters, i.e. the asymptotic mean:

$$P = \lim_{\substack{h \to \infty \\ T \to \infty}} \mathrm{E}\{\overset{a}{P}_k\} \tag{16}$$

and the asymptotic mean square error:

$$e^2 = \lim_{\substack{h \to \infty \\ T \to \infty}} \mathrm{E}\{(\overset{a}{P}_k - P_0)^2\} \tag{17}$$

It can be shown (20–24) that the output of the instruments set up with one of the previously described sampling strategies is asymptotically unbiased ($\overline{P} = P_0$) and, consequently, the asymptotic mean square error coincides with the asymptotic variance $e^2 = \sigma^2$ whose final expression can always be expressed as follows:

$$\sigma^2 = 2\sum_{q=1}^{\infty} |P_q|^2 W^2(q\ f_1 T_s) \tag{18}$$

According to the superposition principle, this equation shows that the contribution of the squared RMS value $2|P_q|^2$ of each harmonic component of the instantaneous power to the asymptotic variance is weighted by the coefficient $W^2(q\ f_1 T_s)$. The sequence of the weighting coefficients $W^2(\ f_1 T_s)$, $W^2(2\ f_1 T_s), \ldots$ can be derived from a continuous weighting function $W^2(\ fT_s)$ by determining its values at the successive occurrence points $\ f_1 T_s, 2\ f_1 T_s$, i.e. the products between each instantaneous-power spectral frequency and the constant lag T_s. Since Eq. (18) is always valid, we can conclude that a corresponding weighting function can be associated with any sampling strategy, recursive or non-recursive, random or equally-spaced, asynchronous or synchronous. Hence the behavior of the weighting function $W^2(\ fT_s)$ as a function of $\ fT_s$ and the possible occurrence points at which the weighting coefficients are evaluated completely describe the performance of any selected sampling strategy with the associated filtering algorithm.

By considering an N-point rectangular window to realize the FIR filter, it can be shown that the weighting function for the sampling strategy defined by Eq. (14) can be expressed as follows:

$$W^2(\ fT_s) = \frac{1}{N} + \mathrm{sinc}^2(2b\ fT_s)[|H(\ fT_s)|^2 - \frac{1}{N}] \qquad (19)$$

where $|H(\ fT_s)|$ is the modulus of the frequency response of the rectangular window (Eq. 9). When $f = 0$ it results $W^2(0) = 1$. For $b = 0$, i.e. an equally spaced sampling, we obviously obtain $W^2(\ fT_s) = |H(\ fT_s)|$; therefore all the previous considerations on this sampling strategy can be deduced also considering the weighting function. For $b > 0$ and $fT_s \geq 1$, the shape of $W^2(\ fT_s)$depends significantly on the given value of b. By selecting $b = 0.5$, i.e. when the random sampling is distributed within an interval equal to the time constant T_s, we obtain:

$$W^2(\ fT_s) \cong \frac{1}{N} \quad \text{for} \quad fT_s \geq 1 \qquad (20)$$

The shape of the weighting functions for $b = 0$ and $b = 0.5$ are represented in Fig. 6-a on the hypothesis of $N = 10$; this very low value of N has been chosen only to show the shape of the weighting function more clearly. We can therefore conclude that the bandwidth of this random sampling strategy with $b = 0$ is not limited by the average sampling frequency $f_s = 1/T_s$, but solely by that of the S/H circuit used. It has been shown that these theoretical findings strongly agree with the experimental ones (25).

The weighting function for the sampling strategy defined by Eq. (15) is the following (26):

$$W^2(\ fT_s) = \frac{1}{N} + \frac{2}{N^2}\sum_{r=1}^{N-1}(N-r)\cos[2\pi r(1+\frac{b}{2})\ fT_s]\mathrm{sinc}^r(b\ fT_s) \qquad (21)$$

The plot of this function for different values of b ($b = 0.5, 1, 2$) and for $N = 10$ is reported in Fig. 6-b. For $f = 0$ we obtain $W^2(0) = 1$, while for $f \to \infty$ it results $W^2(\ fT_s) \to 1/N$; the shape of this weighting function differs from that of the non-recursive one only for the presence of a ripple around $1/N$ whose amplitude decreases as b, i.e. the range of the random increments X_{k-i} in Eq. (15), increases. Clearly, the overshoot above $1/N$ must not exceed an acceptable threshold in order to contain the contribution of each spectral component to the asymptotic variance through the corresponding weighting coefficients; on the other hand, higher values of b increase the mean response time of the wattmeter, and consequently b must be selected as small as possible. An optimum value is $b = 1.5$, but in any case the value of b is not critical. The theoretical study has been confirmed by the experimental results with a prototype implementing this sampling strategy (27).

It is interesting to note that the standard error associated with the sampling strategy and filtering algorithm of both these asynchronous random strategies results $1/\sqrt{N}$while that of the quasi-synchronous equally-spaced one is $1/N$; therefore a large bandwidth in an asynchronous sampling can be obtained only with a decrease in accuracy. Since the bandwidth of the proposed asynchronous random strategies is not limited by the sampling frequency but only by the bandwidth of the S/H, a high resolution ADC can be adopted in order to implement a wattmeter characterized both by a large bandwidth and a high resolution. A prototype based on the strategy defined by Eq. (4) was used to evaluate the power losses in electronic devices used in switching converters. Modern power devices are characterized by low losses and high switching speed. Therefore, the instrument required to measure their power losses must have a bandwidth from dc to several MHz and a resolution so high that its performance is still acceptable when the power factor is of a percent order. The accuracy of the experimental results was of some percent in comparison with that of the calorimetric method (28).

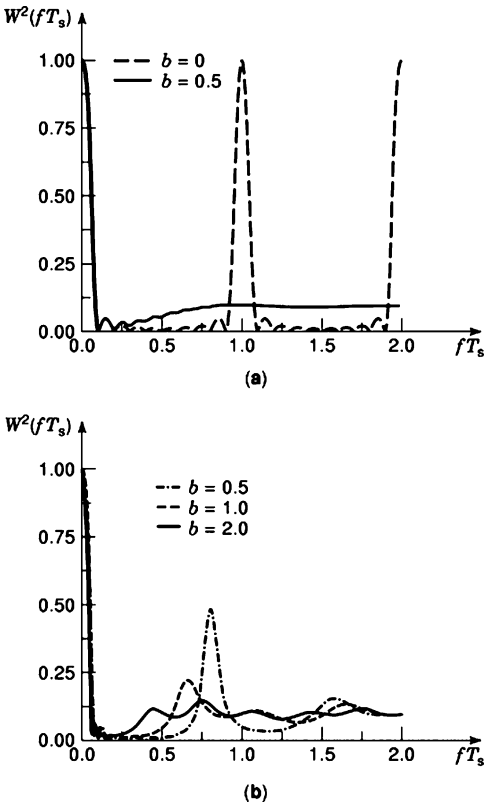

Figure 6. Comparison between the weighting functions of the equally spaced sampling strategy and the random one defined in Eq. (14) with $b = 0.5$ and $N = 10$ (a); weighting function of the random recursive one defined in Eq. (15)(b)

TIME-JITTERED EQUISPACED SAMPLING WATTMETERS

The random fluctuations with respect to the nominal sampling instants are commonly called time-jitter; since they are present both in the voltage and current channels, the effect of time-jitter on the performance of the wattmeter must be considered (29). For instance, the unpredictable temporal variations of the aperture delay of each channel S/H produces different random effects in the sampling instants; the noise associated with the clock generator can instead cause common random independent fluctuations in the sampling instants. Therefore, the effect of time-jitter

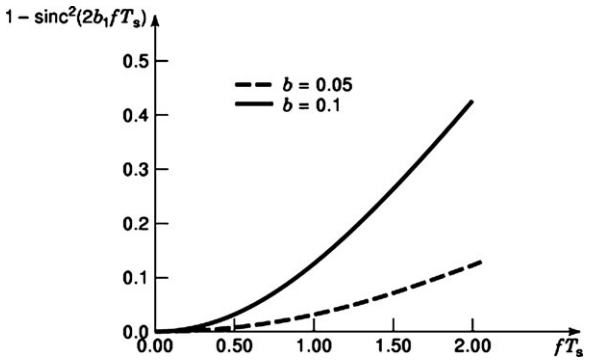

Figure 7. Weighting function of an equally spaced sampling technique with a common time-jitter in the two channels on the hypothesis of $b = 0.05$ or $b = 0.1$ and $N = 10$.

must be analyzed by considering the sampling instants of the two channels separately and each of them can be determined by adding to the right side of Eq. (4) two quantities: $X_{k-i}T_s$, common to the two channels, and $X'_{k-i}T_s$ for the voltage channel or $X''_{k-i}T_s$ for the current channel respectively:

$$t'_{k-i} = \tau_0 + (k - i + X_{k-i} + X'_{k-i})T_s \tag{22}$$

$$t''_{k-i} = \tau_0 + (k - i + X_{k-i} + X''_{k-i})T_s \tag{23}$$

Obviously, t'_{k-i} and t''_{k-i} are mutually interdependent due to the common component X_{k-i}. Each of the three random variables X_{k-i}, X'_{k-i} and X''_{k-i} is the i^{th} element of three independent sets of random variables having a continuous distribution with mean value equal to zero. The two variables X'_i and X''_i can be assumed to be characterized by the same distribution.

In the special case of only common time-jitter having a uniform distribution in a certain interval $\pm b$, the effect of time-jitter can be evaluated by considering the random sampling strategy defined by Eq. (14). Therefore Eq. (19) also represents the weighting function for this case when b has a small value. The shape of the weighting functions $W^2(\ fT_s)$ of an equally spaced sampling strategy with a jitter uniformly distributed within $\pm b = \pm 0.1$, or $\pm b = \pm 0.05$, and $N = 10$ are shown in Fig. 7 (18). This figure shows that time-jitter leads to values of the relative minima increasing with frequency and values of the relative maxima decreasing with frequency. Therefore, in the presence of time-jitter, the contribution of the spectral components that meet the condition $q \neq zN$ must also be investigated in order to limit the asymptotic mean square error. By imposing a maximum value on the weighting function, the upper limit of the wattmeter frequency caused by a given time-jitter can be deduced from Eq. (19) or Fig. 7.

Separate time-jitters for the current a voltage channels generate an asymptotic bias which, under the assumption of periodic input signals and a uniform distribution of the random variables in the interval $\pm b_1$, can be expressed as follows (29):

$$\underset{\rightarrow}{\text{Bias}} = \sum_{\substack{m=-\infty \\ m\neq 0}}^{+\infty} V_m I_m^* (1 - \text{sinc}^2(2b_1 m\ f_1 T_s)) \tag{24}$$

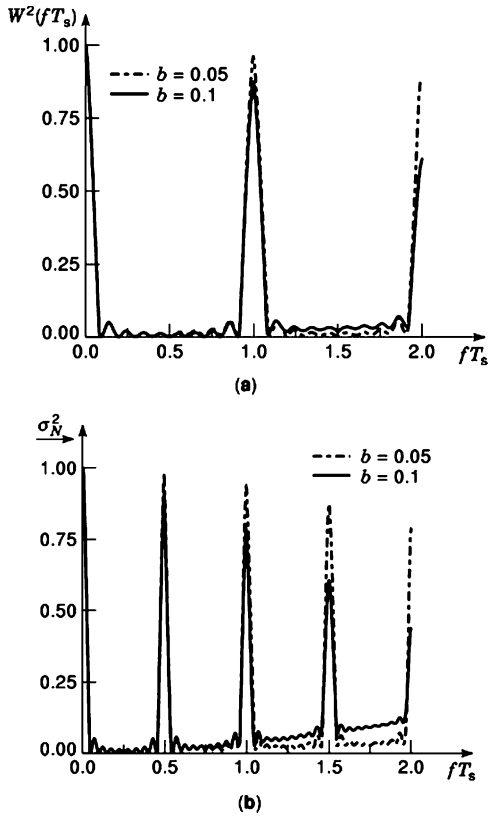

Figure 8. Plots to evaluate the bias (a) and the normalized variance (b) of the wattmeter output in presence of different time-jitters in the two channels on the hypothesis of $b = 0.5$ or $b = 0.1$.

where V_m and I_m with $V_{-m} = V_m^*$, $I_{-m} = I_m^*$ are the spectral components in the exponential form of the input signals and $m\ f_1$ the corresponding frequencies. By Parseval theorem, the average power P_0 can be expressed as a sum of the average power associated with each individual Fourier component of the input signals:

$$P_0 = \sum_{\substack{m=-\infty \\ m\neq 0}}^{+\infty} V_m I_m^* \tag{25}$$

Therefore the asymptotic bias can be obtained by weighting the contribution of each spectral component with the average power and summing over the whole spectrum. Figure 8-a shows the plot of the weight $(1 - \text{sinc}^2(2b_1\ fT_s))$ in Eq. (24) as a function of fT_s for $\pm b_1 = \pm 0.05$ or $\pm b_1 = \pm 0.1$. Therefore, the bias introduces another bandwidth limitation when it becomes comparable with the instrument's accuracy.

The expression of the asymptotic mean square error in the presence of both common and separate time-jitters is rather complex. A more simple result can be deduced when the effect of the common time-jitter is negligible and under the assumption of two sinusoidal input signals at frequency $m\ f_1$. In this case the asymptotic variance can be

expressed as follows (28):

$$\begin{aligned}\overset{2}{\underset{\rightarrow}{\sigma}} &= 2|V_m I_m^*|^2\{\frac{2}{N}(1-\mathrm{sinc}^4(2b_1 m\ f_1 T_s)) \\ &\quad +\mathrm{sinc}^4(2b_1 m\ f_1 T_s)|H(2m\ f_1 T_s)|^2\}+ \\ &\quad +\frac{P_0^2}{2}\{\frac{1}{N}[\mathrm{sinc}^2(4b_1 m\ f_1 T_s)-\mathrm{sinc}^4(2b_1 m\ f_1 T_s)]\}\end{aligned} \tag{26}$$

Figure 8-b shows the shape of the normalized quantity $\sigma_N^2 = \overset{2}{\underset{\rightarrow}{\sigma}} /2|V_m I_m^*|^2$ for in-phase input signals as a function of $\underset{\rightarrow}{f} T_s$ under the assumption of sampling instants uniformly distributed over the interval $\pm b_1 T_s$ with $\pm b_1 = \pm 0.05$ or $\pm b_1 = \pm 0.1$, $N = 10$. The shape of this function is very similar to that of the weighting function in the presence of only common time-jitter (Fig. 9); therefore a further bandwidth limitation is introduced.

In conclusion, the effect of time-jitters in an equally spaced time sampling must be evaluated since it introduces an asymptotic variance and, if different time-jitters exist in the two channels, it also introduce a bias. The instrument bandwidth must therefore be adequately limited in order to make these effects negligible. When one of the two previously described random sampling strategies is considered instead [Eqs. (14) and (15)], only the different time-jitters introduce a further bandwidth limitation.

INPUT CONDITIONING CIRCUITS

The conditioning circuits of Fig. 2 must convert the voltage and current, which the power to be measured depends on, into signals acceptable by the multiplier. When the line voltage is hazardous for the operator, these circuits must also ensure insulation between the instrument and the power system.

The input signals of the multiplier must be of the same type, i.e. either current or voltage, according to the multiplier operating principle. As a consequence, voltage to current (V-I) and current to voltage (I-V) transducers are necessary. The multiplier input signals must also have proper amplitude. This calls for current to current (I-I) and voltage to voltage (V-V) transducers.

All the above transducers could easily be implemented by means of impedances. In this case, the V-I and I-V transducer transfer functions depend on an admittance or an impedance, respectively; while the transfer function of I-I and V-V transducers depend on the ratio between impedances. It is worth recalling that it is easier to know and keep constant the value of an impedance ratio than the value of an impedance. I-I and V-V transducers can be also implemented by means of instrument transformers, which is the most common solution when electrical safety is the main requirement. Broadband thermal rms/dc converters based on thermocouples are used in wattmeters implementing the quarter square technique. However, the frequency bandwidth of such instruments is limited at several orders of magnitude below that of these converters because of the analog circuits that provide the currents $(i_1 + i_2)$ and $(i_1 - i_2)$ appearing in Eq. (2).

Power measurement accuracy depends on the characteristics featured by all the signal conditioning chain; hence, also those of the transducers external to the instrument must be considered.

The choice of a transducer depends on both magnitude and bandwidth of the input quantity. The frequency bandwidth depends on the wattmeter application. For instance, in many industrial processes, where large amounts of power at high currents and voltages are utilized, the active power is substantially transmitted at industrial frequency, even under nonsinusoidal conditions. Indeed, the difference $(P - P_1)$ between the active power P and that at industrial frequency is usually lower than a few parts per thousand of P_1 (30); in particular, the active power associated with the direct voltage and current components can be neglected. In these cases, the use of passive instrument transformers can therefore be quite satisfactory. In other industry applications power measurements may require transducers featuring wider frequency bandwidths (31), also including the direct component.

Resistors

Resistors are a simple and cheap solution for the implementation of the above variety of transducers. Their frequency bandwidth includes the direct component and may range up to about hundred MHz. This means that the output of a resistor based transducer may feature a phase shift of about 0.1 mrad at 10 kHz. The frequency bandwidth is limited by the nominal power of the resistor. Indeed, if the thermal drift is stressed to remain constant, the component sizes must increase as the dissipated power increases, and this increases the resistor time constant. The power dissipation also sets a limit for the use of resistors in self contained instruments. For this reason, external series resistors have been used in electrodynamic wattmeters to extend the voltage range.

The stray parameters may significantly affect the time constants of the resistive voltage divider components. When the two sections of a divider are characterized by different time constants, its transfer function differs from the dc ratio. This is described by means of the ratio and phase-angle errors. The time constants can be compensated by means of capacitors, thus making the division ratio independent of frequency.

Resistor based transducers do not ensure electrical insulation between the power system and the instrument. They involve the use of insulation amplifiers that degrade the transducer metrological performance, which in the case of noninductive shunts would be excellent as for bandwidth and linearity.

Current and voltage transformers

Passive instrument transformers have frequency bandwidth that does not include the direct component and is limited by the stray capacitances. Hence, a current transformer (CT), even for high voltage applications, features a wider frequency bandwidth than a voltage transformer (VT). Usually CTs show satisfactory frequency response in the audio frequency range, while ferrite core CTs may feature upper cut off frequencies of tens of MHz. Broadband I-V transducers can therefore be implemented by means of CTs with resistive burden. Their output, contrary to that of shunt resistors, does not require amplification.

Table 1. Characteristics of two I–V wide bandwidth transducers

Transducer type	Full-scale input (A)	Full.scale output (V)	Cut–off frequencies	Accuracy (%)
Non-inductive shunt resistor	100	0.1	1.5 MHz	±0.1
CT with resistive burden	65	6.5	1 Hz to 20 MHz	−0/+1

Table 1 compares some characteristics of two commercial I-V transducers of similar price. The upper cut off frequency of the VTs depends on their nominal voltage and is usually lower than 1 kHz. A VT can also be implemented by using a CT having nominal input in the order of some mA, suitable resistors in series with the input and a resistive burden. This way, the VT bandwidth can be greatly increased at the cost of a reduction of about one order of magnitude of the nominal input voltage. Both the nominal voltage and the upper cut-off frequency of this solution, which is commonly used to implement active VTs, are mainly limited by the resistor performance.

Active instrument transformers are used when the input signal bandwidth includes the direct component. They contain a sensing element which is usually based on the Hall effect; commercial devices having a saturable inductor as sensing element are also available. In comparison with the instrument transformers based on Hall effect, those using saturable inductors and having similar nominal input ensure higher bandwidth (up to close 1 MHz instead of several kHz, in the case of VTs), better accuracy and linearity.

The ratio error (it is expressed in percent of the nominal input) and the phase-angle error, both defined in the frequency domain, are the parameters characterizing the accuracy of CTs and VTs. Very often data sheets do not give information on the phase-angle error exhibited by active instrument transformers.

Through-type CTs are widely used in industry; their use is necessary when high current values have to be measured. The values of both the ratio and phase-angle errors are influenced if the conductor, which acts as primary turn, is not centered in the transducer window. This detrimental effect is enhanced in the case of through-type CTs containing a flux sensor (the position of the primary conductor with respect to the core joints and the sensor greatly influences the transducer performance). It is greatest in the case of split-core CTs, which allow the current measurement without disconnecting the primary conductor, where the secondary turns are wound on only one leg of the core.

Rogowski coils

Rogowski coils are used to measure currents up to hundreds of kA. A Rogowski coil essentially consists of a toroidal coil placed round the conductor carrying the current to be measured, thus ensuring insulation between the instrument and the power system. The electromotive force induced in the coil is proportional to the time derivative of the current and to the mutual inductance of the coil and the conductor. The current to be measured is obtained by integrating the coil output voltage and by scaling it by the reciprocal of the value of the mutual inductance. The voltage value produced by a Rogowski coil is in the order of 1 μV/Hz for 1 A current flowing in the conductor; this may therefore require amplification.

Specifications of these transducers commonly available on the market are here given by way of example: measuring range up to 10 kA; bandwidth 10 Hz to 100 kHz; accuracy in rms reading not greater than 1%, phase-angle error at 50 Hz: not lower than some tens of mrad; linearity 0.2%.

Given that Rogowski coils have no ferromagnetic material in their core, they cannot be driven into saturation. Therefore, these transducers both have good linearity and are able to measure alternating components of currents having a direct component. Rogowski coils designed to measure alternating components superimposed to a dc of several kA are available.

Coil thickness and width give rise to a contribution to uncertainty depending on the conductor position in the coil cross section. This contribution can be minimized by making the coil turns of an identical cross-sectional area and by uniformly distributing them around a circular path. A split Rogowski coil features a better performance than a split-core CT: a misalignment of the joining coil ends only affects the uncertainty in the current amplitude, not the phase angle error.

Capacitive dividers

Capacitors are the passive components that best approach the ideal behaviour over a wide frequency bandwidth, which is limited by stray resistances and inductances. Capacitive voltage dividers are often used to extend the amplitude range of the multiplier on alternating voltages. The phase shifts exhibited by capacitive dividers depend on the difference between the capacitor loss angles and may be less than 0.1 mrad up to hundreds of kilohertz. At frequencies sufficiently lower than the resonance frequency f_0 depending on the stray inductance, the capacitance of a capacitor is a linear function of the squared ratio of the frequency to f_0. Therefore, if the capacitors possess different resonance frequencies, the voltage division accuracy depends on frequency. Moreover, for direct voltages and for alternating voltages at very low frequency, capacitive dividers cannot be used because of stray phenomena. The dc voltage division is independent of the capacitance values of the two sections and is determined only by their equivalent parallel resistances. At low frequency the voltage division can also be affected by the occurrence of interfacial polarization.

Like all impedance dividers, capacitive dividers do not ensure the isolation of the instrument from the power system; however, high voltage transducers based on them are usually built, given that voltage transformers are too expensive for voltage values greater than about 150 kV. Since the divider output voltage commonly ranges between 5 and 20 kV, they are coupled with a VT that therefore limits the frequency response of the whole conditioning chain.

WATTMETERS CALIBRATION

Calibration is the process of deducing or checking the instrument's accuracy. It can be performed by using either a dedicated calibration equipment (direct comparison) or a similar test instrument of known accuracy used as reference (indirect comparison). The calibration procedure must meet the traceability condition; this means that the individual measurement results must be referred to national standards through an unbroken chain of calibration. Wattmeter calibration is performed at $\cos(\varphi) = 1$ for different amplitude and frequency values; in addition, power factor effects must be taken into account. For the latter effect at least four operating conditions are tested: unity, 0.5 (lead and lag) and zero power factors. For the intercomparison of the results of wattmeter calibration between different Bureaus of Standards, more complex approaches are followed. They provide an estimate of three error coefficients related to the magnitude and phase errors of the voltage and current circuits, and also of zero offset (32).

The first method for calibration (direct comparison) requires synchronized sources of ac voltage and current. To this end voltage and current should be known in amplitude and phase; moreover an adequate range of voltages, currents and phase angle values at different frequencies must be available (33, 34). A single instrument may replace the complex combinations of individual voltage and current sources. If the current and voltage circuits of the wattmeter are supplied by separate sources (phantom loading), the source must provide only the power dissipated into the instrument under test. In order to generate accurate reference signals and separated voltage and current channels, synthesized generators are normally used. A frequency range from 20 Hz up to 10 kHz and a best long term accuracy of less than 100 ppm referred to the apparent power are normally provided in commercial calibrators.

The second method (indirect comparison) compares the readings of the unit under test with those of a reference unit. Also in this case it is preferable that the current and voltage circuits of the wattmeter are supplied from separated sources (phantom loading). If only one power source is available, the calibration can be performed by connecting the voltage channels of the two wattmeters in parallel and connecting the current channels in series with a short-term stable load.

The issues related to electric-power quality have increased the interest in harmonic-power analyzers. Their calibrators offer accuracy and frequency ranges lower than those of the above-mentioned wattmeter calibrators. For instance, a calibration system characterized by an uncertainty of 500 ppm over a frequency bandwidth of about 2 kHz was described in Ref. 35.

POWER QUALITY ANALYZER

The availability of sampled values of the input signals allows further quantities to be computed. The most part of recent digital wattmeters, also in their basic version, provide the measurement of active (average), reactive and apparent power, power factor, energy, frequency and, of course, rms values of current and voltage. As optional function, many of them propose harmonic analysis suites. This opportunity allows several additional parameters to be estimated: harmonic components (magnitude and phase) and total harmonic distortion factor (THD) of both voltage and current and harmonic power, i.e. the contribution of each harmonic component of voltage and current to the active power. Moreover, it must be underlined that, according to the above considerations, the trend is to produce multifunction instruments for the measurement of electrical quantities. Such instruments are usually referred to as power quality analyzers or power quality meters. In addition to the previous parameters, they measure a wide variety of power-quality related quantities: flicker severity, voltage dips and swells, overvoltage, voltage unbalance, short and long interruptions of the voltage are only examples. Some instruments also provide an alert signal and store the data when a certain parameter does not fulfill the limit endorsed by power-quality standards.

BIBLIOGRAPHY

1. W. Mc. Siebert, *Circuits, Signals, and Systems*. McGraw-Hill Book Company, N.Y., 1986.
2. Y. J. Wong, and W. E. Ott, *Function Circuits*. McGraw-Hill Book Company, N.Y., 1976.
3. F. K. Harris, *Electrical Measurements*. J. Wiley & Sons, N.Y., 1952.
4. G. Schuster, Thermal Measurement of AC Power in Comparison with the Electrodynamic Method. *IEEE Trans. Instrum. Meas.*, Vol.**IM-25**, No. 4,December 1976, pp. 529–533.
5. L. G. Cox, and N. L. Kusters, A Differential Thermal Wattmeter for the AC/DC Transfer of Power. *IEEE Trans. Instrum. Meas.*, Vol.**IM-25**, No. 4,December 1976, pp. 553–557.
6. R. Bergeest, and P. Seyfried, Evaluation of the Response of Time-Division Multipliers to AC and DC Input Signals. *IEEE Trans. Instrum. Meas.*, Vol.**IM-24**, No.4,December 1975, pp. 296–299.
7. M. M. Staborowski, Modern Numerical Analysis of Time-Division Multipliers. *IEEE Trans. Instrum. Meas.*, Vol.**IM-28**, No. 1,March 1979, pp. 74–78.
8. G. J. Johnson, Analysis of the Modified Tomota-Sugiyama-Yamaguchi Multiplier. *IEEE Trans. Instrum. Meas.*, Vol.**IM-33**, No. 1,March 1984, pp. 11–16.
9. P. N. Miljanic, B. Stojanovic, and R. Bergeest, Systematic Error of Time-Division Wattmeters when Voltage and/or Current Are Distorted. *IEEE Trans. Instrum. Meas.*, Vol.**IM-36**, No. 2,June 1987, pp. 357–361.
10. P. S. Filipski, A TDM Wattmeter with 0.5-MHz Carrier Frequency. *IEEE Trans. Instrum. Meas.*, Vol.**IM-39**, No. 1,February 1990, pp. 15–18.
11. R. S. Turgel, Digital Wattmeter Using a Sampling Method. *IEEE Trans. Instrum. Meas.*, Vol.**IM-23**, No. 4,December 1974, pp. 337–341.
12. J. J. Hill, and W. E. Alderson, Design of a Microprocessor-Based Digital wattmeter. *IEEE Trans. Ind. Electron. Control Instrum.*, Vol.**IECI-28**, No. 3,August 1981, pp. 180–184.
13. C. F. Coombs, *Electronic Instrument Handbook*(2nd edition). McGraw-Hill, N.Y., 1995.

14. C. H. Dix, Calculated performance of a digital sampling wattmeter using a systematic sampling. *IEE Proc.*Vol.**129**, Pt. A, No. 3,May 1982, pp. 172–175.
15. F. J. J. Clarke and J. R. Stockton, Principle and theory of wattmeters operating on the basis of regularly spaced sample pairs. *J. Phis. E.*, 1982, pp. 645–652.
16. F. Filicori, D. Mirri, and M. Rinaldi, Error estimation in sampling digital wattmeters. *IEE Proc.*Vol.**132**, Pt. A, No 3,May 1985, pp. 122–128.
17. G. N. Stenbakken, A wideband sampling wattmeter. *IEEE Trans. Power Appar. Syst.*, Vol.**PAS-103**, No. 10,October 1984, pp. 2919–2926.
18. D. Mirri, G. Iuculano, F. Filicori, and G. Pasini, Performance Function for Time-Jittered Equispaced Sampling Wattmeters. *IEEE Trans. Instrum. Meas.*, vol.**44**, No. 3,June 1995, pp. 671–674.
19. G. N. Stenbakken, and A. Dolev, High-Accuracy Sampling Wattmeter. *IEEE Trans. Instrum. Meas.*, vol.**41**, No. 6,December 1992, pp. 974–978.
20. F. Filicori, G. Iuculano, A. Menchetti, and D. Mirri, A random asynchronous sampling strategy for measurement instruments based on non-linear signal conversion. *IEE Proc.*, vol.**136**, pt. A, No. 3,May 1989, pp. 141–150.
21. D. Mirri, G. Iuculano, A. Menchetti, F. Filicori, and M. Catelani, Recursive Random Sampling Strategy for a Digital Wattmeter. *IEEE Trans. Instrum. Meas.*, December 1992, vol.**41**, No. 6,pp. 979–984.
22. G. E. P. Box, and G. C. Tiao, *Bayesian Inference in Statistical Analysis*. Addison-Wesley, New York, 1973.
23. F. Filicori, G. Iuculano, A. Menchetti, D. Mirri and M. Catelani, New performance function for the comparison of different sampling strategies in non-linear conversion instruments. *Proceedings of IEEE Trans. Instrum. and Meas. Technol. Conf.*, Washington, April 1989, pp. 307–311.
24. G. Iuculano, D. Mirri, F. Filicori, A. Menchetti and M. Catelani, A criterion for the analysis of synchronous and asynchronous sampling instruments based on non linear processing. *IEE Proc.*, vol.**139**, part A, No. 4,July 1992, pp. 141–152.
25. D. Mirri, F. Filicori, G. Iuculano, and A. Menchetti, Efficient implementation of digital measurement instruments by random asynchronous sampling. IMEKO TC4 Symp. "Measurement in Electrical and Electronic Power Systems", *Zurich*, September 1989, pp. 231–240.
26. D. Mirri, G. Iuculano, A. Menchetti, F. Filicori, and M. Catelani, Recursive Random Sampling Strategy for a Digital Wattmeter. *IEEE Trans. Instrum. and Meas.*, December 1992, vol.**41**, No. 6,pp. 979–984.
27. A. Menchetti, D. Mirri, G. Pasini, and G. Iuculano, A wideband random-sampling wattmeter. IMEKO TC4 Symp. "Intelligent instrumentation for remote and on-site measurements", Brussels, May 1993, pp. 355–361.
28. A. Menchetti, D. Mirri, G. Pasini, F. Filicori, G. Iuculano: Power loss measurements in electronic switching devices using a new type of digital wattmeter. *Proceedings of IMEKO XII-World Congress on "Measurement and Progress", Pechino (Cina)*,September 1991, pp. 1118–1123.
29. D. Mirri, G. Pasini, G. Iuculano, F. Filicori, and D. Pritelli,Experimental results in a time-jittered equally-spaced sampling wattmeter. IMEKO TC4 Symp. "New Measurement and Calibration Methods of Electrical Quantities and Instruments", Budapest, September 1996, pp. 259–262.
30. IEEE Working Group on nonsinusoidal situations, Practical definitions for powers in systems with nonsinusoidal waveforms and unbalanced loads: a discussion, *IEEE Trans. Power Deliv.*, Vol.**11**, No. 1,January 1996, pp. 79–101.
31. K. C. Kenneth, D. T. Hess, A 1000 A/20 kV/25 kHz-500 kHz Volt-Ampere-Wattmeter for Loads with Power Factors from 0.001 to 1.00, *IEEE Trans. Instrum. Meas.*, Vol.**45**, No. 1,February 1996, pp. 142–145.
32. W. J. M. Moore, E. So, N. M. Oldham, P. N. Miljanic and R. Bergeest, An international comparison of power meter calibrations conducted in 1987. *IEEE Trans. Instrum. Meas.*, Vol.**38**, No. 2,April 1989, pp. 395–401.
33. A. Gubisch, P. L. Lualdi, P. N. Miljanic, and J. L. West, Power calibration using sampled feedback for current and voltage. *IEEE Trans. Instrum. and Meas.*, Vol.**46**, No. 2,April 1997, pp. 403–407.
34. N. Miljanic, Calibrator for alternating voltage, current and power. *IEEE Trans. Instrum. Meas.*, Vol.**38**, No. 2,April 1989, pp. 384–389.
35. R. Arseneau, and P. Filipski, A calibration system for evaluating the performance of harmonic power analyzers. *IEEE Trans. Power Deliv.*, Vol.**10**, No. 3,July 1995, pp. 1177–1182.

DOMENICO MIRRI
GAETANO PASINI
GAETANO IUCULANO
FABIO FILICORI
RENATO SASDELLI
ROBERTO TINARELLI
Dipartimento di Ingegneria Elettrica Università di Bologna, Viale Risorgimento, 2, Bologna, Italy
Dipartimento di Ingegneria Elettronica Università di Firenze, Via Santa Marta, 3, Firenze, Italy
Dipartimento di Elettronica, Informatica e Sistemistica Università di Bologna, Viale Risorgimento, 2, Bologna, Italy